Eur. Phys. J. D **31**, 3–10 (2004)
DOI: 10.1140/epjd/e2004-00118-y

THE EUROPEAN PHYSICAL JOURNAL D

# Continuous-wave Doppler-free two-photon spectroscopy of the $4d^{10}5s\ ^2S_{1/2} \rightarrow 4d^95s^2\ ^2D_{3/2}$ transition in atomic silver

T. Badr[1], M.D. Plimmer[1,a], P. Juncar[1], M.E. Himbert[1], J.D. Silver[2], and G.D. Rovera[3]

[1] BNM-INM, CNAM[b], EA 2367, 292 rue Saint-Martin, 75003 Paris, France
[2] Clarendon Laboratory, Parks Road, Oxford OX1 3PU, UK
[3] BNM-SYRTE, 61 avenue de l'Observatoire, 75014 Paris, France

Received 21 April 2004
Published online 7 September 2004 – 

**Abstract.** The frequencies of the hyperfine components of the transition $4d^{10}5s\ ^2S_{1/2} \rightarrow 4d^95s^2\ ^2D_{3/2}$ in $^{107}$Ag and $^{109}$Ag have been determined using Doppler-free two-photon laser spectroscopy of a thermal atomic beam and heterodyne calibration with respect to a molecular iodine line 111R(18-1) near 520 THz. For the centre of gravity of a mixture of natural abundance, we deduce the value 1 040 706 327(3) MHz. For the isotope shift, we obtain $\nu(^{109}\mathrm{Ag}) - \nu(^{107}\mathrm{Ag}) = +599.6(2)$ MHz. We find the magnetic hyperfine splitting constants of the excited state to be $A(^{107}\mathrm{Ag}\ (^2D_{3/2})) = -315.9(2)$ MHz and $A(^{109}\mathrm{Ag}\ (^2D_{3/2})) = -363.3(2)$ MHz, an order of magnitude improvement over previous authors [W. Fischer et al., Z. Phys. **238**, 249 (1970)].

**PACS.** 06.20.Fn Units and standards – 06.30.Ft Time and frequency – 32.10.Fn Fine and hyperfine structure – 32.30.Jc Visible and ultraviolet spectra – 32.60.+i Zeeman and Stark effects

## 1 Introduction

The silver atom is an interesting candidate for an optical frequency standard based on narrow two-photon transitions from the $4d^{10}5s\ ^2S_{1/2}$ ground state (Fig. 1). Excitation of the $4d^95s^2\ ^2D_{3/2}$ state, whose natural width is about 4 kHz, requires two photons near 576 nm. Detection of this transition via cascade fluorescence is straightforward. The narrower $4d^95s^2\ ^2D_{5/2}$ level (natural width less than 1 Hz) can be excited using two photons near 661 nm and was first proposed as a frequency standard in 1976 [1]. This transition is harder to detect because the upper level is metastable. More recently, the group of Walther at the Max Planck Institut für Quantenoptik, Garching, has cooled and trapped a sample of silver atoms using the $5s\ ^2S_{1/2} \rightarrow 5p\ ^2P_{3/2}$ transition at 328 nm [2]. In our own laboratory, we employ a thermal atomic beam with a first aim of observing both two-photon transitions as a prelude to laser cooling work.

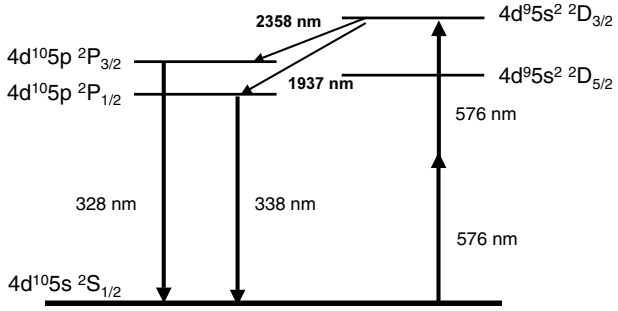


**Fig. 1.** Partial energy level diagram for Ag I showing the transitions of interest.

## 2 Current experiment

In this article, we describe a measurement of the frequency, isotope shift and hyperfine structure of the $4d^{10}5s\ ^2S_{1/2} \rightarrow 4d^95s^2\ ^2D_{3/2}$ transition using Doppler-free two-photon laser spectroscopy. Our aim was to perform a pilot experiment to test the performance of our laser system, power build-up cavity, light collection optics and atomic beam apparatus for a narrow transition without the need to detect metastable atoms. For a given homogeneous linewidth, the excitation probability per unit laser power squared is expected to be similar for double quantum excitation of the $4d^95s^2\ ^2D_{3/2}$ and $4d^95s^2\ ^2D_{5/2}$ states. This is demonstrated by calculations based on the Cowan codes [3]. In other words, successful excitation of

[a] e-mail: Mark.Plimmer@ne.ch
*Present address*: Observatoire cantonal, rue de l'observatoire 58, 2000 Neuchâtel, Switzerland.
[b] Website: http://www.cnam.fr/instituts/inm/

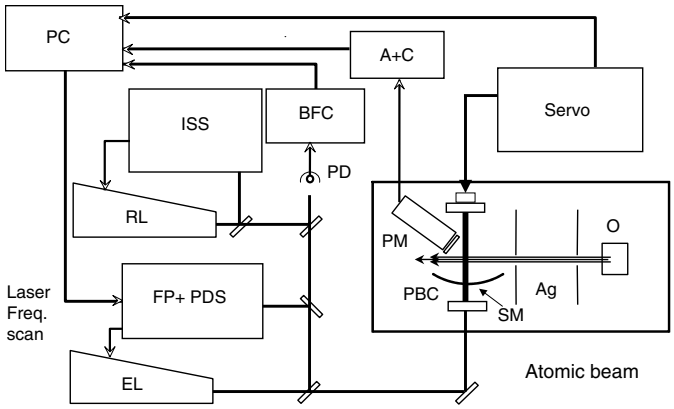


**Fig. 2.** Experimental set-up. A = amplifier, C = counter, EL = excitation laser, RL = reference laser, ISS = iodine saturation spectrometer, PD = photodiode, BFC = beat frequency counter, FP = Fabry Perot cavity, O = oven, PBC = power build-up cavity, PC = personal computer, PDS = Pound-Drever servo, PM = photomultiplier tube, SM = spherical mirror. In reality, the PM, protected by a colour glass filter is located directly above the interacton region, perpendicular to the page and the SM below.

the former transition would be a stepping stone to the observation of the latter[1].

## 2.1 Apparatus

The apparatus is shown in Figure 2. One laser excites the silver transition in the atomic beam while the frequency of a second dye laser is servo-locked to the hyperfine component $a_3$ of the line 111R(18−1) in molecular iodine ($^{127}I_2$) using saturated absorption spectroscopy. The beat signal between the two lasers measured by a counter (HP 5131A) provides direct calibration of the frequency axis. The whole experiment is controlled by a personal computer via an interface (National Instruments) with a program written in LabView.

### 2.1.1 Atomic beam

The atomic beam unit is similar to that described in [4] except that since we work with ground state atoms, the electron gun is switched off. Three 100 $ls^{-1}$ turbo-molecular pumps (Alcatel for the source, Pfeiffer TPH 260 for the middle and detection regions) backed by diaphragm pumps (Balzers MZ2T for the oven and intermediate chambers and MD4T for the detection chamber) provide an oil-free vacuum around $4 \times 10^{-6}$ mbar in the source chamber, $10^{-6}$ mbar in the middle and $10^{-7}$ mbar in the detection region under running conditions. Damping bellows between the turbo-molecular pumps and the main body of the vacuum housing reduce the transmission of vibrations to the power build-up cavity described below (Sect. 2.1.4).

[1] *Note added in proof:* Shortly after submission of this article, two-photon excitation of the $^2D_{s/2}$ level was indeed observed in our laboratory.

### 2.1.2 Excitation laser

The laser used to probe the silver transition is a Coherent model 699-21 continuous ring dye laser using rhodamine 6G dye pumped by a 6 W $Ar^+$ ion laser at 514.5 nm. We use a Radiant Dyes high pressure dye nozzle and circulator (10 bar) and cool the reservoir to around +6 °C. The same pump laser drives the reference dye laser described in the next section. Frequency jitter is reduced by the use of an intra-cavity electro-optic actuator (Gsänger 0202) and a fast electronic servo. A microwave sideband method [5] is used to lock the output frequency of the laser to the centre of a fringe of a hemiconfocal Fabry Perot ($FP$) cavity (finesse 600 at 576 nm). The error signal gave an estimate of the frequency jitter with respect to the cavity of below 10 kHz for a 1 s integration time. The cavity of length 50 cm, diameter 8 cm, formed by two fused silica mirrors optically adhered to a Zerodur spacer, is placed in a sealed enclosure under vacuum (0.1 mbar). We scan the laser frequency by varying the length of the $FP$ cavity, one of whose mirrors is mounted on a deformable Zerodur structure compressed by a piezo-electric stack. A potential difference of 1500 V applied to the latter allows one to change the frequency by a free spectral range (300 MHz). The frequency is measured to within 30 MHz using a wavemeter (Burleigh model WA 1500) and more finely via the beat signal with the reference laser described immediately below.

### 2.1.3 Reference laser

This reference laser is a second Coherent 699-21 ring dye laser, frequency stabilised with its commercial standard servo electronics and dye circulator since the requirements on laser jitter are less stringent than for the excitation laser. However, a filter of type Eurofiltec DF4E 0.45N has proved essential to reduce an unacceptable amount of dye bubbles and associated frequency fluctuations. An external acousto-optic modulator (A&A-DTS 75-125, $f$ = 100 MHz) is used to modulate the pump beam in the saturated absorption spectrometer (modulation frequency 15 kHz, amplitude 2 MHz). We lock the frequency of this laser to that of the hyperfine component $a_3$ of the line 111R(18-1) in $^{127}I_2$. The latter is observed using saturated absorption spectroscopy in a glass cell of length 50 cm, whose cold point is maintained at a temperature 8.0(1) °C. A typical iodine spectrum is shown in Figure 3.

### 2.1.4 Power build-up cavity

To increase the two-photon transition probability, proportional to the square of the laser intensity, as well as to ensure overlap of the counter-propagating laser beams, a FP cavity (length 145 mm, finesse 300) is placed in the vacuum chamber around the interaction region. The length of the cavity was servo-locked to maintain resonance with the laser frequency using a 17 kHz dither of the output mirror

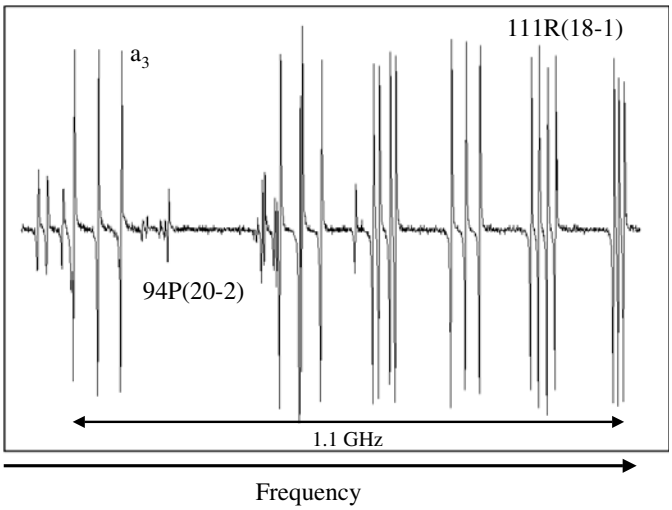


**Fig. 3.** First derivative spectrum of a scan over the $^{127}I_2$ line 111R(18-1) showing the hyperfine component $a_3$ used for frequency calibration of silver two-photon spectra. The smaller resonances are due to the line 94P(20-2).

and phase sensitive detection of the transmitted light intensity (Stanford Research Systems model SR830 lock-in amplifier). In this way we could obtain intra-cavity powers of over 12 W for a dye laser output power of 300 mW. The discrepancy between this value and the theoretical amplification factor of 100 is explained by coupling losses. In our first observations of the transition, both mirrors had a reflectivity $R = 99\%$ and radii of curvature 100 mm, giving a beam waist $w_0 = 90$ $\mu$m. Subsequently, to reduce transit-time broadening, we increased $w_0$ to 340 $\mu$m, using mirrors of radius of curvature 10 m.

#### 2.1.5 Detection scheme

We detected the fluorescence at 328 and 338 nm resulting from the cascade decay via the $5p\ ^2P_{3/2}$ and $5p\ ^2P_{1/2}$ levels using a 50 mm diameter photomultiplier tube (PM) in pulse counting mode (Hamamatsu $R5113P$ — quantum efficiency 0.25) and 2 colour glass filters (Schott type $UG11$, thickness 3 mm) embedded in plasticine to block light leaks. The latter were preferred to an interference filter because the fluorescence is smeared out over about 2.5 cm given the 40 $\mu$s lifetime of the $4d^9 5s^2\ ^2D_{3/2}$ level and mean atomic velocity of 660 m s$^{-1}$. A spherical mirror, radius of curvature 10 cm, diameter 9 cm, was placed 3 cm below the interaction region to increase the light collection efficiency. The pulses from the PM were sent via a high-speed amplifier (Stanford Research Systems SR445 (gain 25)) to a counter (Stanford Research Systems SR400). A typical background count rate of 50 000 s$^{-1}$ arose from unfiltered oven light. The noise on this background, a few hundred counts per second, is negligible in comparison with the signals observed.

## 3 Experimental procedure and data analysis

To estimate a priori the transition frequencies to find the resonances we used Fourier transform measurements by Nave [6] of the lines at 1937 and 2358 nm, combined with those of Pickering and Zilio at 328 and 338 nm [7]. Using the measured hyperfine splittings of the $5s\ ^2S_{1/2}$ [8], $5p\ ^2P_{1/2}$ [9], $5p\ ^2P_{3/2}$ [10] and $5s^2\ ^2D_{3/2}$ states [11], the isotope shift at 328 nm [2] and thereby estimating that at 338 nm [12], we localised positions of hyperfine components in each isotope (Tab. 1). We scan the excitation laser frequency over about 4 MHz around each hyperfine component of the transition for the two stable isotopes $^{107}$Ag and $^{109}$Ag. Since the first-order Doppler effect is eliminated, the angle between the laser and atomic beams has a negligible impact on the measured excitation frequency. We record the fluorescence count, the transmitted power from the build-up cavity as well as the beat frequency between the excitation and reference lasers. The results of scans over different isotopes and hyperfine components are combined later to deduce isotope shift and the different hyperfine splitting constants. Ideally, to evaluate the light shift, proportional to the laser intensity, we would like to have acquired data for a series of different laser powers and fixed geometry. In practice, we used measurements at two different laser beam diameters differing by a factor four, i.e. a factor of 16 in intensity. We did this because, in order to resolve two hyperfine components in different isotopes which, accidentally, lie only ≈800 kHz apart (Fig. 4), we needed to increase the beam diameter to reduce transit time broadening. Typical single-photon linewidths were then 500−600 kHz. Although the theoretical lineshape arising from transit-time and Zeeman broadening is somewhat complicated, to analyse the data, we fitted either Lorentzian or Gaussian profiles to the individual components. Where Zeeman components were partially resolved ($F = 1 \rightarrow F' = 1$), a sum of Lorentzian profiles gave the best fit, i.e. the lowest residuals (Fig. 4). By contrast, with unresolved Zeeman substructure ($F = 0 \rightarrow F' = 2$, or $F = 1 \rightarrow F' = 2$), we obtained a much better fit with a single Gaussian curve (Fig. 5). Even so, the centre frequencies varied by less than 10 kHz even if Lorentzian curves were used. The symmetric Doppler broadened background due to absorption of co-propagating photons was ignored. Given the excellent signal to noise ratio (>300) limited by photon statistics, we could find line centres to within 10−20 kHz.

## 4 Systematic effects

In the following sections we discuss the various perturbations affecting the values of the transition frequencies, hyperfine splitting constants and isotope shift. An error budget is given in Table 2. The accuracy of the frequency of the $^{127}I_2$ reference line, deduced using the IodineSpec program from TOPTICA is considered by its developers to be 1.5 MHz [13]. The first-order Doppler shift is absent because we use counter-propagating laser beams and excitation occurs at the beam waist. The second-order Doppler

**Table 1.** Measured frequencies in megahertz of the hyperfine components of the transition $4d^{10}5s\ ^2\mathrm{S}_{1/2}\ F \rightarrow 4d^9 5s^2\ ^2\mathrm{D}_{3/2}\ F'$ in Ag I. The labels 328, 338, 1937 and 2358 refer to the wavelengths in nanometres of the transitions used to estimate a priori the frequencies. Here measurements at 1937 and 2358 nm are by Nave [6] and those at 328 and 338 nm by Pickering and Zilio [7]. To calculate positions of hyperfine components in each isotope from their measurements, we used the measured hyperfine splittings of the $5s\ ^2\mathrm{S}_{1/2}$, [8] $5p\ ^2\mathrm{P}_{1/2}$ [9], $5p\ ^2\mathrm{P}_{3/2}$ [10] and $5s^2\ ^2\mathrm{D}_{3/2}$ states [11], the isotope shift at 328 nm [2] and used the latter to estimate that at 338 nm [12].

| Isotope | $F$ | $F'$ | Frequency $-\,1\,040\,704\,000$ MHz | | |
|---|---|---|---|---|---|
| | | | This work | 328+2358 | 338+1937 |
| $^{107}$Ag | 0 | 2 | 516.6(3.0) | 653(32) | 630(32) |
| $^{107}$Ag | 1 | 2 | 2229.2(3.0) | 2366(32) | 2343(32) |
| $^{107}$Ag | 1 | 1 | 2860.9(3.0) | 2992(37) | 2962(32) |
| $^{107}$Ag | centroid | | 2038.0(3.0) | 2173(32) | 2146(32) |
| $^{109}$Ag | 0 | 2 | 882.4(3.0) | 1023(32) | 989(32) |
| $^{109}$Ag | 1 | 2 | 2859.3(3.0) | 3000(32) | 2966(32) |
| $^{109}$Ag | 1 | 1 | 3585.9(3.0) | 3711(35) | 3691(32) |
| $^{109}$Ag | centroid | | 2637.6(3.0) | 2773(32) | 2744(32) |
| $^{109}$Ag, $^{107}$Ag | centroid of both | | 2326.8(3.0) | 2461(32) | 2435(32) |

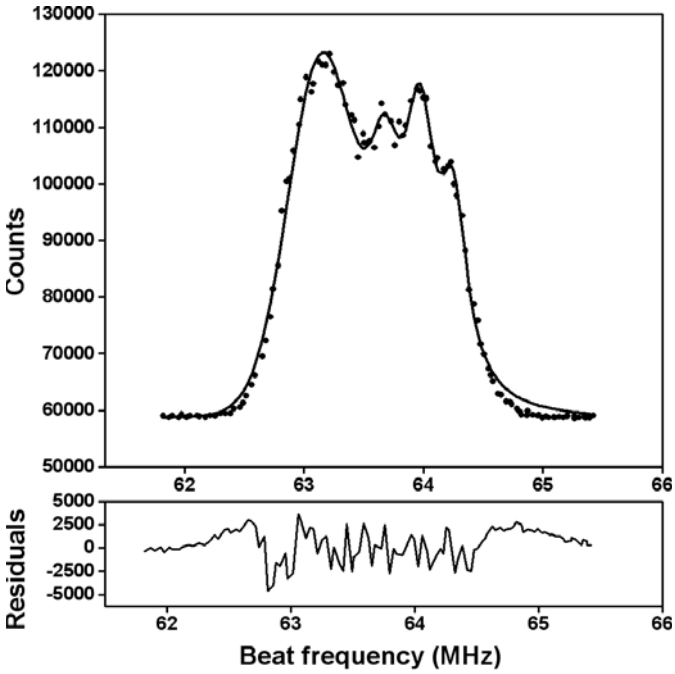


**Fig. 4.** Scan over two hyperfine components of the transition $4d^{10}5s\ ^2\mathrm{S}_{1/2}\ F \rightarrow 4d^9 5s^2\ ^2\mathrm{D}_{3/2}\ F'$ in atomic silver. The closely spaced resonances shown are $F = 1 \rightarrow F' = 1$ in $^{107}$Ag and $F = 1 \rightarrow F' = 2$ in $^{109}$Ag. The dots represent experimental data and the solid curve is a superposition of a fitted Gaussian (left) and 3 Lorentzian (right) profiles. The residuals are shown underneath.

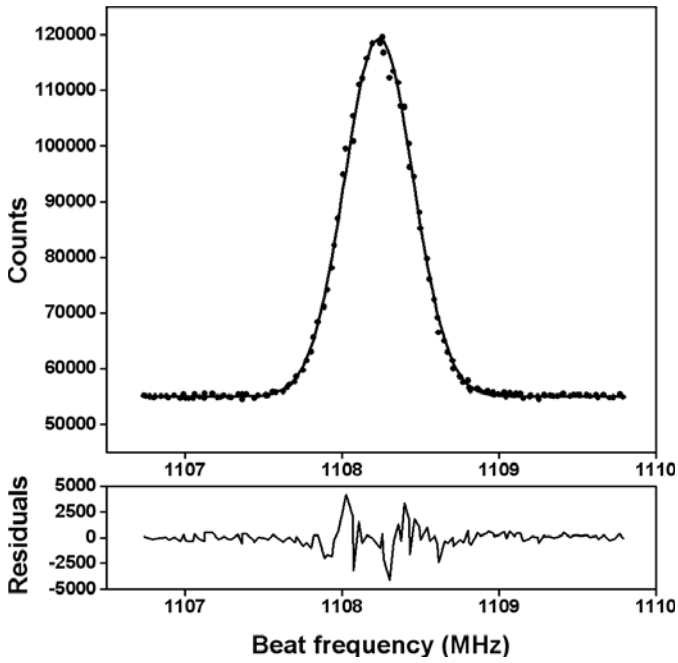


**Fig. 5.** Scan over the hyperfine component $4d^{10}5s\ ^2\mathrm{S}_{1/2}\ F = 0 \rightarrow 4d^9 5s^2\ ^2\mathrm{D}_{3/2}\ F' = 2$ in $^{107}$Ag. The dots represent experimental data and the solid curve a fitted Gaussian profile. The residuals are shown underneath.

shift, about 1 kHz for our thermal beam (most probable velocity 660 ms$^{-1}$) is negligible. The D.C. Stark shift is even more negligible than for the case of the 547.7 nm line, discussed in our earlier paper [4]. In fact, only two atomic perturbations have any importance at our level of accuracy: the light shift due to the excitation laser, and the Zeeman shift. A further consideration is the lock point of the reference laser. We chose the component $a_3$ of the iodine reference line because it is well separated from other components (Fig. 3) and thus symmetrical about line centre. Drifts of the cell temperature (≈500 Hz/°C) have a negligible effect upon the frequency compared with the uncertainty of the iodine line itself.

### 4.1 Light shift

The a.c. Stark shift due to the off-resonant interaction of the excitation laser with the silver atoms is an oft-cited

**Table 2.** Sources of uncertainty in the determination of frequencies of hyperfine components of the transition $4d^{10}5s\ ^2\mathrm{S}_{1/2}\ F \rightarrow 4d^9 5s^2\ ^2\mathrm{D}_{3/2}\ F'$ in atomic silver.

| Quantity at twice the laser frequency | Contribution to absolute frequency (kHz) | Contribution to hyperfine splitting constants (kHz) |
|---|---|---|
| Frequency of $^{127}\mathrm{I}_2$ reference line 111R(18-1) | 3000 | 0 |
| Reference laser lock point | <50 | <70 |
| Determination of centroid | 100 | 140 |
| Zeeman shift (1st order) (residual circular polarisation) | 70 | 100 |
| Zeeman shift (2nd order) | ≈1 | <1 |
| Light shift ($P = 10$ W) | 15 | 5 |
| D.C. Stark shift | <1 | <1 |
| Second-order Doppler shift | <1 | ≪1 |
| Quadratic sum | 3000 | 180 |

drawback of two-photon spectroscopy. In the case of the present transition, the light shift is estimated to be about −250 kHz for 10 W and $w_0 = 90$ $\mu$m, which represents about a sixth of the linewidth. Even this value would contribute only a small error to the value of the frequency of each hyperfine component. In the calculation of the hyperfine splittings, all that counts is the differential light shift, five times smaller. Furthermore, the data used to calculate final values were taken with a beam waist of $w = 340$ $\mu$m, for which the light shift of about 16 kHz is comparable with curve fitting uncertainties.

### 4.2 Zeeman effect

Because we did not plan to obtain linewidths as narrow as those observed, we neither shielded nor compensated the ambient magnetic field, measured to be 500(50) mG using a 3-axis Hall effect probe (Bartington model MAG 03-MC). As expected, the Zeeman effect leads to a splitting of the components of the $(F = 1 - F' = 1)$ and $(F = 1 - F' = 2)$ transitions, evidence for which can be seen in Figure 4. Since we use linearly polarised light, this splitting should be symmetric and lead to a broadening but no overall shift of the line centre to first order. However, because there is an angle of ≈ 30° between the vertical electric vector of the laser and the magnetic field, the component $(F = 0 - F' = 2)$ is also broadened. This is supported by the fact that we obtained only a two-fold reduction in linewidth (1.2 MHz to 600 kHz) when the beam diameter was expanded by a factor of four. In addition, the existence of several components for the transition $F = 1 - F' = 1$ can only be explained if transitions with $\Delta M_F = \pm 1$ occur, since both levels have $g_F = 1$ (Tab. 3). Furthermore, since we cannot exclude a degree of residual circular polarisation within the power build-up cavity, there remains the possibility of a small first-order Zeeman shift. We take 50 kHz as a conservative upper limit.

We should like to point out that because both $^{107}$Ag and $^{109}$Ag have a nuclear spin $I = 1/2$, it is possible to obtain an expression for the Zeeman effect of the hyperfine structure which is valid to all orders of magnetic field strength. (It can be deduced from the Breit-Rabi formula applicable for $J = 1/2$ [14,15] using the substitutions $I \leftrightarrow J$ and $g_J \leftrightarrow -g'_I$). Specifically, the shift $\Delta E$ of the magnetic sub-level $|I, JM_I, M_J\rangle$ caused by a magnetic flux density $B$ is given by

$$\Delta E = -\frac{h\Delta\nu}{2(2J+1)} + g_J\mu_B BM \pm \frac{h\Delta\nu}{2}\sqrt{1 - \frac{4Mx}{2J+1} + x^2} \tag{1}$$

where $h\Delta\nu$ is the energy separation between the two hyperfine levels in zero magnetic field, $M = M_I + M_J$ and the parameter $x$ is given by

$$x = \frac{\mu_B B(g_J + g'_I)}{h\Delta\nu}. \tag{2}$$

Since there are at least 30 stable isotopes of various elements with nuclear spin $I = 1/2$, this rarely presented result may be of wider interest. In the weak field limit, $x \rightarrow 0$, we recover the usual expression for the Zeeman shift of the hyperfine level $|F, M_F\rangle$:

$$\Delta E = g_F\mu_B BM_F. \tag{3}$$

**Table 3.** Landé factors $g_F$ for the hyperfine components of the transition $4d^{10}5s\ ^2\mathrm{S}_{1/2}\ F \rightarrow 4d^9 5s^2\ ^2\mathrm{D}_{3/2}\ F'$ in atomic silver. For simplicity, we have taken $g_S = 2$ and neglected $g'_I$.

| Level | $^2\mathrm{S}_{1/2}$ | | $^2\mathrm{D}_{3/2}$ | |
|---|---|---|---|---|
| $F$ | 0 | 1 | 1 | 2 |
| $g_F$ | 0 | 1 | 1 | 3/5 |

## 5 Results and discussion

We measured individually the frequencies of the three hyperfine components for the stable isotopes $^{107}$Ag and $^{109}$Ag. From their separations we calculated the hyperfine splittings of the ground and excited states and hence the magnetic dipole hyperfine constants $A$. The difference

**Table 4.** Measured values in megahertz of the magnetic dipole hyperfine coupling constants $A$ for the levels $4d^{10}5s\ ^2\mathrm{S}_{1/2}$ and $4d^9 5s^2\ ^2\mathrm{D}_{3/2}$ in $^{107}$Ag and $^{109}$Ag.

| Level | Isotope | This work | Other authors | Reference |
|---|---|---|---|---|
| $4d^{10}5s\ ^2\mathrm{S}_{1/2}$ | $^{107}$Ag | −1712.54(18) | −1712.512111(18) | [8] |
| | $^{109}$Ag | −1976.85(18) | −1976.932075(17) | [8] |
| $4d^9 5s^2\ ^2\mathrm{D}_{3/2}$ | $^{107}$Ag | −315.9(2) | −315.7(1.6) | [8,11] |
| | $^{109}$Ag | −363.3(2) | −363.1(1.8) | [11] |

of the centres of gravity for each isotope gave the isotope shift. Finally, to compare our results with previously published values, we calculated the centre of gravity of the spectrum of a naturally abundant sample containing 51.84% $^{107}$Ag and 48.16% $^{109}$Ag. The results are shown in Tables 1 and 4. The most delicate part of the analysis was correct identification of hyperfine components, in particular the closely spaced doublet discussed above (Fig. 4). At first sight, the larger peak would appear to be due to the more abundant isotope $^{107}$Ag. On closer inspection, it is in fact due to $^{109}$Ag: the first-order Zeeman shift causes a greater splitting of the resonance in $^{107}$Ag, and thus the height to diminish. A critical test is provided by comparison with the hyperfine constants of the ground state $5s\ ^2\mathrm{S}_{1/2}$. Our values lie within 80 kHz of the far more accurate radio-frequency measurements of Dahmen and Penselin [8], a difference smaller than our error bar. Our values for the excited state $4d^9 5s^2\ ^2\mathrm{D}_{3/2}$ hyperfine constant are about an order of magnitude more accurate than those of Fischer et al. [9,11] with which they agree. Our measurements enable the first direct determination of the isotope shift of the transition. The value we find 599.6(0.2) MHz agrees remarkably well with that we estimated from the sum of isotope shifts of the lines at 328 nm [2] and 2358 nm [6], namely 599.5(16.0) MHz.

By contrast, as regards the optical frequency of the transition (1 040 706 327(3) MHz) there is no close agreement with other measured values deduced from Fourier transform spectroscopy of hollow cathode discharge emission lines (Tab. 1). Our uncertainty of 3.0 MHz is dominated by that of the molecular iodine reference line. The disagreement with the value of Pickering and Zilio [7] (34 714.305(7) $\mathrm{cm}^{-1}$ = 1 040 708 682(210) MHz a difference of 2 GHz or 10 standard deviations) confirms their suspicion of problems due to line blending with the argon buffer gas spectrum [16,17]. A much earlier value from the literature (34 714.16 $\mathrm{cm}^{-1}$ = 1 040 704 335 MHz), [18], lies even further away. Finally, our values lie about 120 MHz below those deduced from recent measurements of the frequencies of the lines at 328 and 338 nm [7] and 1937 and 2358 nm [6] whose respective standard uncertainties are given as about 30 and 10 MHz.

## 6 Conclusion

We have performed measurements of the frequency, isotope shift and hyperfine structure of the $4d^{10}5s\ ^2\mathrm{S}_{1/2} \rightarrow 4d^9 5s^2\ ^2\mathrm{D}_{3/2}$ transition in atomic silver. As far as we are aware, this work marks the first observation of a two-photon transition from the ground state of this atom. Moreover, for a given laser power and experimental resolution, the signal-to-noise ratio (>300 in 1 s) is expected to be similar for excitation of the much narrower transition $4d^{10}5s\ ^2\mathrm{S}_{1/2} \rightarrow 4d^9 5s^2\ ^2\mathrm{D}_{5/2}$ and this work can be regarded as an encouraging step towards a study of the latter. Our measurement of the frequency, obtained using laser heterodyne techniques lies about 120 MHz below values deduced from measurements of different transitions by other authors using Fourier transform spectroscopy [6,7]. We have performed the first direct measurement of the isotope shift of this transition. Our value is compatible with those estimated by comparison with other transitions in silver [2,9]. Our values for the hyperfine splitting constants of the $4d^9 5s^2\ ^2\mathrm{D}_{3/2}$ level are eight times more accurate than those of previous results [9,11].

The authors are deeply indebted to G. Nave for providing results prior to publication and are grateful to D.J.E. Knight for critical reading of the manuscript. We thank J. Fodor for modelling optics with a view to increasing fluorescence collection. J.D.S. thanks the *Conservatoire National des Arts et Métiers* and *the Bureau National de Métrologie* for visiting fellowships. This work was supported in part by the *Bureau National de Métrologie*.

## Appendix

Here we calculate the frequencies of hyperfine components of the transitions

(a) $4d^9 5s^2\ ^2\mathrm{D}_{3/2} \rightarrow 4d^{10}5p^2\ ^2\mathrm{P}_{3/2}$ at $\lambda = 2358$ nm;
(b) $4d^9 5s^2\ ^2\mathrm{D}_{3/2} \rightarrow 4d^{10}5p^2\ ^2\mathrm{P}_{1/2}$ at $\lambda = 1937$ nm;
(c) $4d^{10}5p\ ^2\mathrm{P}_{3/2} \rightarrow 4d^{10}5s\ ^2\mathrm{S}_{1/2}$ at $\lambda = 328$ nm;
(d) $4d^{10}5p\ ^2\mathrm{P}_{1/2} \rightarrow 4d^{10}5s\ ^2\mathrm{S}_{1/2}$ at $\lambda = 338$ nm.

For comparison with other authors, we give the centres of gravity of each isotope, the isotope shift and the centre of gravity of a mixture of natural abundance.

### A.1 $4d^9 5s^2\ ^2\mathrm{D}_{3/2} \rightarrow 4d^{10}5p^2\ ^2\mathrm{P}_{3/2}$ at $\lambda = 2358$ nm

We use the recent measurement of Nave [6] in which only the hyperfine structure of the $5s^2\ ^2\mathrm{D}_{3/2}$ level was resolved. For the splitting of the $5p\ ^2\mathrm{P}_{3/2}$, we take the value of

**Table 5.** Frequencies in megahertz of the hyperfine components of the transition $4d^9 5s^2\ ^2\mathrm{D}_{3/2}\ F \rightarrow 4d^{10}5p\ ^2\mathrm{P}_{3/2}\ F'$ at $\lambda = 2358$ nm in Ag I deduced from measurements by [6,8,10].

| Isotope | $F$ | $F'$ | Frequency $-127\,157\,000$ MHz |
|---|---|---|---|
| $^{107}$Ag | 2 | 1 | 15(12) |
| $^{107}$Ag | 2 | 2 | 79(12) |
| $^{107}$Ag | 1 | 1 | 641(21) |
| $^{107}$Ag | 1 | 2 | 705(21) |
| $^{107}$Ag | centroid | | 290(9) |
| $^{109}$Ag | 2 | 1 | 1053(12) |
| $^{109}$Ag | 2 | 2 | 1127(12) |
| $^{109}$Ag | 1 | 1 | 1764(18) |
| $^{109}$Ag | 1 | 2 | 1838(18) |
| $^{109}$Ag | centroid | | 1366(8) |
| $^{109}$Ag, $^{107}$Ag | centroid of both | | 1808(6) |

**Table 6.** Frequencies (in megahertz) of the hyperfine components of the transition $4d^9 5s^2\ ^2\mathrm{D}_{3/2}\ F \rightarrow 4d^{10}5p^2\ ^2\mathrm{P}_{1/2}\ F'$ at $\lambda = 1937$ nm in Ag I deduced from measurements of [6,8,11].

| Isotope | $F$ | $F'$ | Frequency $-154\,757\,000$ MHz |
|---|---|---|---|
| $^{107}$Ag | 2 | 1 | 230(3) |
| $^{107}$Ag | 1 | 0 | 674(6) |
| $^{107}$Ag | 1 | 1 | 849(6) |
| $^{107}$Ag | centroid | | 418(3) |
| $^{109}$Ag | 2 | 1 | 1267(3) |
| $^{109}$Ag | 1 | 0 | 1791(6) |
| $^{109}$Ag | 1 | 1 | 1992(6) |
| $^{109}$Ag | centroid | | 1489(4) |
| $^{109}$Ag, $^{107}$Ag | centroid of both | | 934(3) |

$A(^{109}\mathrm{Ag}) = -37$ MHz due to Carlsson et al. [10] and calculate that in $^{107}$Ag using the ratio of the $4d^{10}5s\ ^2\mathrm{S}_{1/2}$ hyperfine splittings and neglecting the hyperfine anomaly. The results are shown in Table 5.

### A.2 $4d^9 5s^2\ ^2\mathrm{D}_{3/2} \rightarrow 4d^{10}5p^2\ ^2\mathrm{P}_{1/2}$ at $\lambda = 1937$ nm

We use another recent measurement of Nave [6] in which only the hyperfine structure of the $5s^2\ ^2\mathrm{D}_{3/2}$ level was resolved. For the splitting of the $^2\mathrm{P}_{1/2}$, we take the value of $A(^{109}\mathrm{Ag}) = -210.4(3.0)$ MHz due to Fischer et al. [11] and calculate that in $^{107}$Ag using the ratio of the $4d^{10}5s\ ^2\mathrm{S}_{1/2}$ hyperfine splittings and neglecting the hyperfine anomaly. The results are shown in Table 6.

### A.3 $4d^{10}5p\ ^2\mathrm{P}_{3/2} \rightarrow 4d^{10}5s\ ^2\mathrm{S}_{1/2}$ at $\lambda = 328$ nm

This transition is used for laser cooling of silver. The frequency of the centre of gravity of a naturally occurring mixture has been measured by Pickering and Zilio [7], and the isotope shift ($-476(10)$ MHz) by Uhlenberg et al. [2]. The ground state hyperfine splittings are due to Dahmen and Penselin [8] and excited state ones are obtained from Carlsson et al. [10] as discussed above.

**Table 7.** Frequencies in megahertz of the hyperfine components of the transition $4d^{10}5p\ ^2\mathrm{P}_{3/2}\ F \rightarrow 4d^{10}5s\ ^2\mathrm{S}_{1/2}\ F'$ at $\lambda = 328$ nm in Ag I deduced from measurements of [2,7,8,10].

| Isotope | $F$ | $F'$ | Frequency $-913\,546\,000$ MHz |
|---|---|---|---|
| $^{107}$Ag | 1 | 0 | 1638(31) |
| $^{107}$Ag | 2 | 1 | 3287(31) |
| $^{107}$Ag | 1 | 1 | 3351(31) |
| $^{107}$Ag | centroid | | 2883(31) |
| $^{109}$Ag | 1 | 0 | 970(31) |
| $^{109}$Ag | 2 | 1 | 2873(31) |
| $^{109}$Ag | 1 | 1 | 2947(31) |
| $^{109}$Ag | centroid | | 2407(31) |
| $^{109}$Ag, $^{107}$Ag | centroid of both | | 2653(30) |

**Table 8.** Frequencies in megahertz of the hyperfine components of the transition $4d^{10}5p\ ^2\mathrm{P}_{1/2}\ F \rightarrow 4d^{10}5s\ ^2\mathrm{S}_{1/2}\ F'$ at $\lambda = 338$ nm in Ag I deduced from measurements of [2,7,8,10,12].

| Isotope | $F$ | $F'$ | Frequency $-885\,946\,000$ MHz |
|---|---|---|---|
| $^{107}$Ag | 1 | 0 | 1400(31) |
| $^{107}$Ag | 1 | 1 | 3113(31) |
| $^{107}$Ag | 0 | 1 | 3888(31) |
| $^{107}$Ag | centroid | | 2728(31) |
| $^{109}$Ag | 1 | 0 | 722(31) |
| $^{109}$Ag | 1 | 1 | 2699(31) |
| $^{109}$Ag | 0 | 1 | 2901(31) |
| $^{109}$Ag | centroid | | 2255(31) |
| $^{109}$Ag, $^{107}$Ag | centroid of both | | 2501(30) |

**Table 9.** Calculated Landé factors of the hyperfine levels involved in the transition $4d^{10}5s\ ^2\mathrm{S}_{1/2} \rightarrow 4d^9 5s^2\ ^2\mathrm{D}_{3/2}$. For simplicity, we have taken $g_S = 2$ and neglected $g'_I$.

| Level | $g_F$ |
|---|---|
| $^2\mathrm{S}_{1/2}\ F = 0$ | 0 |
| $^2\mathrm{S}_{1/2}\ F = 1$ | 1 |
| $^2\mathrm{D}_{3/2}\ F' = 1$ | 6/5 |
| $^2\mathrm{D}_{3/2}\ F' = 2$ | 3/5 |

### A.4 $4d^{10}5p\ ^2\mathrm{P}_{1/2} \rightarrow 4d^{10}5s\ ^2\mathrm{S}_{1/2}$ at $\lambda = 338$ nm

This transition could be employed for repumping during laser cooling of silver. The frequency of the centre of gravity of a naturally occurring mixture has been measured

by Pickering and Zilio [7]. To deduce the isotope shift (−479(12) MHz), we assume the same field shift as that for the 328 nm line [2] and estimate the specific mass shift using the formula of Heilig and Steudel [12]. Ground state hyperfine splittings are due to Dahmen and Penselin [8] and excited state are obtained from Fischer et al. [11] as discussed above.

## References


1. P.L. Bender, J.L. Hall, R.H. Garstang, F.M.J. Pichanick, W.W. Smith, R.L. Barger, J.B. West, Bull. Am. Phys. Soc. **21**, 599 (1976)
2. G. Uhlenberg, J. Dirscherl, H. Walther, Phys. Rev. A **62**(6), 063404–1 (2000)
3. R.D. Cowan, *The Theory of Atomic Structure and Spectra* (University of California Press, Berkeley, 1981)
4. S. Guérandel, T. Badr, M.D. Plimmer, P. Juncar, M.E. Himbert, Eur. Phys. J. D **10**, 33 (2000)
5. R.W.P. Drever, J.L. Hall, F.V. Kowalski, J. Hough, G.M. Ford, A.J. Munley, H. Ward, Appl. Phys. B **31**, 97 (1983)
6. G. Nave, private communcation, 2003
7. J.C. Pickering, V. Zilio, Eur. Phys. J. D **13**, 181 (2001)
8. H. Dahmen, S. Penselin, Z. Phys. **200**, 456 (1967)
9. W. Fischer, H. Hühnemann, E. Krüger, Z. Phys. **216**, 136 (1968)
10. J. Carlsson, P. Jönsson, L. Störesson, Z. Phys. D **16**, 87 (1990)
11. W. Fischer, H. Hühnemann, Th. Meier, Z. Phys. **238**, 249 (1970)
12. K. Heilig, A. Steudel, At. Data Nucl. Tables **14**, 613 (1974)
13. H. Knoeckel, `www.toptica.com` and private communication, 2003
14. G. Breit, I.I. Rabi, Phys. Rev. **38**, 2082–2083, 1931
15. S. Millman, I.I. Rabi, J.R. Zacharias, Phys. Rev. **53**, 384 (1938)
16. W. Whaling, W.H.C. Anderson, M.T. Carle, J.W. Brault, H.A. Zarem, J. Res. Natl. Inst. Stand. Technol. **107**, 149 (2002)
17. J.C. Pickering, private communication, 2003
18. E. Rasmussen, Det. Kgl. Danske Videnskab., Math-fys. Medd. (Copenhagen) **18**, 1 (1940)